The Visual Triple Star ADS 16185 - STF2934

Henry Zirm

Markt Schwaben, Bavaria
Germany

henryzirm@gmx.de

Abstract: In this article the visual triple star ADS 16185 - STF2934 is examined. In first studies by Heintz in 1962 and 1981 were reported a probably, up to now unresolved third star. As with similar visual multiple star systems like Zeta Aquarii or Zeta Cancri, a periodic "wobble" in the measurements of the apparent outer orbit (the visible components) is clearly visible. With the help of extensive, additional visual and speckle measurements from the past 30 years, an improvement of the outer (visible component) and inner (invisible component) orbit was performed.

Introduction

This system is located in Pegasus and was first observed by H.G.W. Struve in 1830. Later, Heintz (1962) was the first observer who held a third, unseen companion in this system very likely. Altogether, there are currently only two complete orbit calculations for an inner and outer orbit, both investigations are from Heintz (1962, 1981).

Adopted from the SIMBAD database, the most relevant designations are: ADS 16185, STF2934, WDS 22419+2126 AB, HIP 112063, HD 215013.

The component A and B has visual magnitudes 8.6 and 9.5 mag. The combined spectral class is G0, information regarding the luminosity class could not be found.

The recalculated Hipparcos trigonometric parallax is 11.35 ± 1.18 mas (van Leeuwen, 2007), this corresponds to a distance of 88 ± 8 parsecs. Tokovin (2002; 2008) published a series of radial velocities for both components. Thereby both components are measured spectroscopically separated. Due to the relatively rapid variation in the radial velocity of the component A, the association of the inner orbit to component A is likely. The radial velocity difference between component B and A defines the position of the ascending node.

Measurements preparation and assignation of weights

The observations used in this work mainly came from the Washington Double Star catalogue (WDS), obtained via email request by Brian D. Mason and his colleagues.

Before using any analytical method to calculate orbital motion parameters, θ was corrected for precession. Furthermore θ and ρ were plotted against time which allows for the detection of measures with important errors or quadrant ambiguity. Measures with the largest errors, provided that these are recognizable as such, were assigned zero weight.

The initial weights for θ and ρ measures were assigned using a the weighting scheme based on Hart-

The Visual Triple Star ADS 16185 - STF2934

kopf, McAlister & Franz (1989), Mason, Douglass Hartkopf (1999), Seymour et al. (2002) for the speckle measures and Docobo & Ling (2003) for the visual measures. The initial θ weights were five times larger than ρ weights (Heintz 1978) for visual measures.

For the chosen orbital calculation, the transformation of θ and ρ into Cartesian coordinates is necessary and follows the guidelines of Heintz (1978). The difference of the measurement accuracy of the angle compared with measurement accuracy of the distance (for the visual measurements) should also be considered in determining the weights. With the help of a weighting transformation, the advantage of this information will be applied. A good way to transform the weights for polar coordinates into weights for Cartesian coordinates was described by van den Bos (1932) and will be here used:

$$\frac{1}{w_\delta} = \frac{\sin^2\theta}{w_\theta} + \frac{\cos^2\theta}{w_\rho} \quad \text{and} \quad \frac{1}{w_\alpha} = \frac{\cos^2\theta}{w_\theta} + \frac{\sin^2\theta}{w_\rho}$$

After several iterations on the basis of a preliminary orbit calculation process, the measures with residuals larger than 3σ were assigned zero weight. Later, the non -zero weight measures were re-assigned following the work of Irwin, Yang & Walker (1996).

Furthermore, to reduce the computational effort, I will calculate "normal points". Here I follow the guidelines to Zirm (2011).

Method of Orbital calculation in general

With direct reference to the method of Hartkopf, McAlister & Franz (1989)), if the three elements, the period **P** (in years), the time of periastron passage **T** and the numerical eccentricity **e** are known; the Thiele-Innes elements (A, B, F, G) can be calculated with a method of least squares (on basis of a given set of observations) with the following formulas:

$$\left.\begin{aligned} x_i &= \rho_i \cos\theta_i = [A]X_i + [F]Y_i \\ y_i &= \rho_i \sin\theta_i = [B]X_i + [G]Y_i \end{aligned}\right\} \qquad \left\{\begin{aligned} X_i &= \cos E_i - e \\ Y_i &= \sqrt{1-e^2}\sin E_i \end{aligned}\right.$$

The geometrical elements, that is, the so-called Campbell-elements (the angular semi major axis (a), inclination (i), position angle of the line of nodes (Ω), and the angle between the node and periastron (ω)) are computed from the Thiele-Innes elements (in rectangular brackets) by a "least square method".

The relationship is described by:

$$\begin{aligned} A &= a(\cos\omega_B \cos\Omega - \sin\omega_B \sin\Omega \cos i) \\ B &= a(\cos\omega_B \sin\Omega + \sin\omega_B \cos\Omega \cos i) \\ F &= a(-\sin\omega_B \cos\Omega - \cos\omega_B \sin\Omega \cos i) \\ G &= a(-\sin\omega_B \sin\Omega + \cos\omega_B \cos\Omega \cos i) \end{aligned}$$

With the following formulae (Argyle 2004) one can transform the Thiele-Innes elements into the Campbell elements:

$$2u = \frac{A^2 + B^2 + F^2 + G^2}{2}; \qquad v = AG - BF$$

$$a^2 = u + \sqrt{(u+v)(u-v)}$$

$$i = \arccos\left(\frac{m}{a^2}\right)$$

$$\omega = \frac{\arctan\dfrac{B-F}{A+G} + \arctan\dfrac{-B-F}{A-G}}{2}$$

$$\Omega = \frac{\arctan\dfrac{B-F}{A+G} - \arctan\dfrac{-B-F}{A-G}}{2}$$

The remaining elements, the period **P** in years, the time of periastron passage **T**, the numerical eccentricity **e** are associated within the following formula; the Kepler equation:

$$\frac{360}{P}(t_i - T) = M_i = E_i - e\sin E_i$$

Heintz (1978) recommends solving the Kepler's equation, the following iterative approximation method. Six iterations are sufficient for obtaining the Eccentric anomaly **E**:

$$E_0 = M + e\sin M + \frac{e^2}{2}\sin 2M$$

$$M_0 = E_0 - e\sin E_0 \qquad E_1 = E_0 + \frac{(M - M_0)}{(1 - e\cos E_0)}$$

The Visual Triple Star ADS 16185 - STF2934

The initial parameter for P, T and e can be adopted from a recently known orbit (in this case from Heintz (1981)) to calculating initial values for E. On this basis, it is now possible to calculate the theoretical positions and to match these with the observed positions of the components.

$$x_{calc} = AX + FY \qquad y_{calc} = BX + GY$$

$$\theta_{calc} = \arctan \frac{-(AX + FY)}{(BX + GY)}$$

$$\rho_{calc} = \sqrt{(AX + FY)^2 + (BX + GY)^2}$$

$$\Delta\theta_i = (\theta_{obs} - \theta_{calc})_i \qquad \Delta\rho_i = (\rho_{obs} - \rho_{calc})_i$$

Calculation of the combined outer and inner orbital motion, adoption for a triple star solution

The following indices are used: AB corresponds to the outer system; Aa corresponds to the inner system. A combined solution for the inner and outer orbital (sub) motion can calculate the corresponding A, B, F, G values from the combined least square equation:

$$x_i = [A_{AB}]X_{AB} + [F_{AB}]Y_{AB} - [A_{Aa}]X_{Aa} - [F_{Aa}]Y_{Aa}$$

$$y_i = [B_{AB}]X_{AB} + [G_{AB}]Y_{AB} - [B_{Aa}]X_{Aa} - [G_{Aa}]Y_{Aa}$$

The residuals $\Delta\theta_i$ and $\Delta\rho_i$ are determining by the followed formulae:

$$X_{AB} = \cos E_{ABi} - e_{AB} \qquad Y_{AB} = \sqrt{1 - e_{AB}^2}\sin E_{ABi}$$
$$X_{Aa} = \cos E_{Aai} - e_{Aa} \qquad Y_{Aa} = \sqrt{1 - e_{Aa}^2}\sin E_{Aai}$$

$$x_{calci} = A_{AB}X_{ABi} + F_{AB}Y_{ABi} - A_{Aa}X_{Aai} - F_{Aa}Y_{Aai}$$
$$y_{calci} = B_{AB}X_{ABi} + G_{AB}Y_{ABi} - B_{Aa}X_{Aai} - G_{Aa}Y_{Aai}$$

$$\theta_{calci} = \arctan \frac{-(A_{AB}X_{ABi} + F_{AB}Y_{ABi} - A_{Aa}X_{Aai} - F_{Aa}Y_{Aai})}{B_{AB}X_{ABi} + G_{AB}Y_{ABi} - B_{Aa}X_{Aai} - G_{Aa}Y_{Aai}}$$

$$\rho_{calci} = \sqrt{\begin{matrix}(A_{AB}X_{ABi} + F_{AB}Y_{ABi} - A_{Aa}X_{Aai} - F_{Aa}Y_{Aai})^2 + \\ +(B_{AB}X_{ABi} + G_{AB}Y_{ABi} - B_{Aa}X_{Aai} - G_{Aa}Y_{Aai})^2\end{matrix}}$$

$$\Delta\theta_i = (\theta_{obs} - \theta_{calc})_i \qquad \Delta\rho_i = (\rho_{obs} - \rho_{calc})_i$$

Process to find the "best orbit"

The theoretical basis of the so called "three dimensional" grid search method follows according to Hartkopf, McAlister, & Franz (1989): "… perform a "three dimensional" grid search in the vicinity of a set of input values of P, T, and e, in each grid step calculating the remaining elements and determining an overall residual…".

Within reasonable limits of P, T, and e, one must now in preselected step sizes adjust the values for P, T, and e in order to obtain the set with the smallest residuals. In that case the value χ^2/ν has to be minimized:

$$\chi^2/\nu = \frac{\sum_{i-1}^{n} w_{\vartheta_i}(\rho_i \Delta\theta_i)^2 + \sum_{i-1}^{n} w_{\rho_i}\Delta\rho_i^2}{2n - 7}$$

The orbit with smallest χ^2/ν value is the orbit with minimum residuals and thus the "best orbit".

The calculation was carried out in Visual Basic (VBA), applied in Microsoft EXCEL2010®. This VBA code was kindly provided by my colleague Francisco Rica Romero.

Results of combined orbit calculation

Starting from the recent elements of Heintz (1981), I now attempt to find the orbit with the lowest residuals by the variation of the dynamic elements P, T, and e. Here, different options have been tried. First, the orbital periods determined by Heintz were used to calculate preliminary circular orbits. The resulting elements a, i, ω, and Ω (2nd column of table 1) were compared with the original elements of Heintz (1st column of table 1). Alone this preliminary calculation yielded a significant reduction of systematic deviations of Heintz orbits.

The next step is the assumption of a circular orbit for the inner and outer system. Now, by alternating variation of P_{inner} and P_{outer} periods, it was searched for the orbital solutions with the lowest χ^2/ν. The resulting elements are written in the 3rd column of Table 1. Also here again a significant improvement can be obtained. But still remained are significant and periodic residuals that were identical with the period of the inner orbit. Derived from this, the inner orbit seems to be eccentric.

For a new "grid search" passageway, the outer orbit is already assumed to be circular, and the inner orbit is

(Continued on page 218)

The Visual Triple Star ADS 16185 - STF2934

Table 1: Collection of calculated orbits, corresponding residuals and masses

	Heintz (1981) original elements	fixed Periods from Heintz (1981)	circular inner and outer orbit	circular outer orbit, eccentric inner orbit	final inner and outer orbit
Orbital elements for the outer orbit AB					
P [yr]	636	636	747	739	**3350**
T [yr]	1769 (2087)	1764.8	1741.3	1740	**1868.6**
e	0	0	0	0	**0.70**
a ["]	1.46	1.48	1.71	1.70	**3.78**
i [°]	126.9	126.7	120.4	119.2	**128.5**
ω [°]	0	0	0	0	**32.0**
Ω_{2000} [°]	207.1[1] (27.1)	210.4[1]	206.9[1]	207.8[1]	**185.5**[1]
Orbital elements for the inner orbit Aa					
P [yr]	82	82	79.3	81.8	**81.0**
T [yr]	2006 (1965)	2005	2001.08	1992.5	**1992.3**
e	0	0	0	0.42	**0.47**
a ["]	0.074	0.099	0.095	0.101	**0.101**
i [°]	42.2	45.8	50.9	55.5	**58.4**
ω_p [°]	0	0	0	308.8	**308.9**
Ω_{2000} [°]	193.8[1] (13.8)	210.3[1]	194.9[1]	198.2[1]	**199.3**[1]
Residuals: χ^2/ν, rms and MA					
χ^2/ν	12.701	2.175	1.635	1.152	**1.000**
rms ϑ [°]	1.52	0.97	0.85	0.74	**0.67**
rms ρ ["]	0.071	0.024	0.021	0.018	**0.017**
MA ϑ [°]	1.28	0.71	0.58	0.43	**0.40**
MA ρ ["]	0.066	0.015	0.015	0.010	**0.010**
Total mass of the system					
ΣM_{AB}	5.3	5.5	6.1	6.2	**3.3**

1. defined due the radial velocity difference adopted from Tokovinin (2002, 2008)

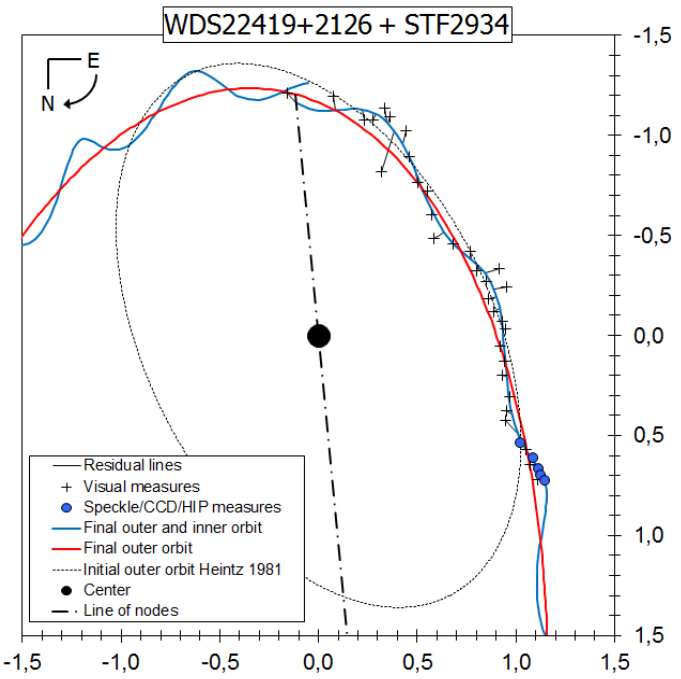

Figure 1: zoomed view of the final orbits and additionally the outer orbital path recently calculated by Heintz (1981). The scale is in arc seconds.

The Visual Triple Star ADS 16185 - STF2934

(Continued from page 216)

assumed to be eccentric. Thereby iterative P_{outer} is searched, then P_{inner}, T_{inner} and e_{inner}. This leads to an improvement of the residuals, supporting the assumption of an eccentric inner orbit. It is known that the assumption of a circular orbit is only a simplification, however the present measurements are not sufficient and cover only a small part of the orbital path and it is very difficult to calculate an eccentric orbit. Therefore the simplification using a circular orbit.

This raises the question: are the present measurements sufficient to calculate a (probably) eccentric outer orbit? The alternating "grid search" variation of P, T, e for the outer and inner orbit, resulted in the "Final Orbit" (Table 1, last column), displayed in a zoomed view in Figure 1.

In principle the result seems to show a convergence to increasing period and eccentricity. However, since the improvement of the $\chi^2/\ \nu$ value, due the changes greater than e ~ 0.7 and P ~ 3500 years, is less than 1 per thousand and it can be terminated at this point. Therefore, the final orbital elements represent quite a good fit on the basis of the currently available measurements. The ephemerides until to 2050 are tabulated in Table 2.

Table 2: Inner and outer orbit Ephemerides

t	$\vartheta°_{2000}$	ρ"
2013.0	53.6	1.275
2014.0	53.2	1.284
2015.0	52.9	1.294
2016.0	52.5	1.303
2017.0	52.2	1.313
2018.0	51.8	1.323
2019.0	51.5	1.333
2020.0	51.2	1.343
2025.0	49.7	1.395
2030.0	48.4	1.449
2035.0	47.2	1.504
2040.0	46.1	1.559
2045.0	45.1	1.614
2050.0	44.2	1.668

Measurements and Residuals

Table 3 gives the historical measurements of STF2934 as obtained from U.S.N.O. Washington Double Star catalogue (WDS). Explanation of reference codes (column 5) can be found on the USNO web site (http://ad.usno.navy.mil/wds/request.html). The last two columns give the differences in position angle (Δθ) and separation (Δρ) from the fitted orbit.

Summary

In this work, final orbital elements for the outer and invisible inner orbit of ADS16185 were determined. A significant reduction of the residuals was obtained in comparison with previous and/or circular orbits. Unfortunately the outer orbit is still too uncertain to obtain a reliable total mass ΣM_{AB} (with correspondingly small errors) for the whole system. It will be important that future observing sessions detect directly the invisible component. The outlook for the upcoming GAIA mission generates hope for the absolute confirmation that ADS16185 is threefold.

Acknowledgements

I am particularly grateful to Francisco Rica Romero for providing a short-term measurement and his very helpful support, he generated the "grid search" algorithm in VBA code. I would like to thank Cliff Ashcraft for his kind support for the correction of the English translation.

This research has made use of the Washington Double Star Catalog maintained at the U.S. Naval Observatory, the NASA Astrophysics Data System Bibliographic Services and the SIMBAD database (operated at CDS, Strasbourg, France).

References

Argyle, B., 2004, Observing and measuring visual double stars, Patrick Moore's practical astronomy series. Berlin: Springer, ISBN: 1852335580

Docobo, J. A.; Ling, J. F., 2003, A&A, 409, 989

Hartkopf, W. I., McAlister, H. A., Franz, O. G., 1989, AJ, 98, 1014

Heintz, W. D., 1978, Double Stars (revised edition), Dordrecht, D. Reidel Publishing Co. (Geophysics and Astrophysics Monographs. Volume 15).

Heintz, W.D, 1962, VeMun, 5, 135H

Heintz, W.D, 1981, ApJS, 45, 559H

(Continued on page 220)

The Visual Triple Star ADS 16185 - STF2934

Table 3: Normal point visual measurements

Date	ϑ°	ρ"	N	Reference	Δ ϑ°	Δ ρ"
1830.780	187.8	1.220	3	StF3	2.1	0.057
1843.420	176.7	1.196	3	Mad3	0.6	0.066
1856.870	168.2	1.100	2	Se_2	-1.1	-0.050
1865.870	166.0	1.110	5	D__4 Frr1	0.5	-0.034
1873.835	163.7	1.183	5	WS_4 Gld1	1.5	0.062
1874.840	162.0	1.150	3	WS_3	0.2	0.033
1879.875	158.8	0.879	8	Sbk2 Hod3 Smt3	-0.7	-0.213
1886.400	156.6	1.114	14	Eng7 dBl2 StH2 Hl_3	0.5	0.066
1891.410	153.0	1.008	27	StH7 Cel2 Sp_8 Com6 Nst2 Glp2	-0.1	0.003
1896.920	146.8	0.914	12	L__1 Cls3 Dys1 Cow1 Bow4 Bry2	-2.1	-0.036
1901.900	142.6	0.907	19	Coh1 Bow10 L__3 Fay1 Hu_1 Pos1 Dob2	-1.2	0.013
1906.915	136.7	0.831	7	Bow2 Frm1 Loh1 L__1 VBs2	0.0	-0.012
1911.200	129.7	0.760	14	Bow11 Wz_3	0.5	-0.059
1916.710	124.2	0.820	14	Dob5 Doo3 Com4 VBs2	3.1	-0.014
1922.115	118.9	0.879	20	Btz5 Cha4 StG6 Dob1 Gcb1 VBs3	2.6	0.016
1926.375	112.3	0.864	25	StG6 B__3 Pav1 Plq1 Els4 Cul1 Rab5 Fur4	-1.1	-0.018
1931.650	110.1	0.973	27	Kui3 Dob2 Fen2 Ol_4 Smw9 Brt3 StG4	-0.3	0.073
1936.955	107.9	0.890	39	Rab14 Baz4 Ol_7 Smw3 Dur7 Dic4	0.4	-0.022
1941.855	104.4	0.986	26	Scd2 Rab20 Vou3 Ard1	-0.4	0.066
1946.450	102.1	0.878	13	Dur4 Baz3 Nev1 Rab3 Ard2	0.0	-0.046
1952.420	97.8	0.895	33	VBs3 Rab20 Dom5 Ol_2 Dju3	-0.6	-0.032
1957.115	94.5	0.935	34	Rab19 Cou6 Wor3 B__3 Dom2 Pau1	-0.6	0.005
1961.660	92.2	0.949	42	Dom2 Wor8 Hei19 VBs5 Sym4 B__4	0.4	0.016
1967.110	86.8	0.921	8	Zul1 Pop1 Wor3 Hei3	-0.5	-0.019
1972.515	82.2	0.953	10	Zul2 Baz3 Wor4 Ole1	-0.2	-0.001
1977.205	77.9	0.953	23	Zul6 Hei9 Hln3 Wor3 Pop2	0.1	-0.021
1981.925	72.6	1.017	35	Hei4 Zul13 Pop5 Wor4 Drd2 Mss4 LBu3	-0.2	0.008
1986.170	68.5	1.023	17	Sca4 Wor3 Zul5 Lin3 Hei2	0.3	-0.034
1990.565	66.0	1.040	13	Zul5 Gii2 Pop1 Hei3 LBu2	2.1	-0.088
1995.940	61.5	1.198	5	Hei3 Alz2	0.9	-0.026
2000.350	58.9	1.253	8	Alz6 Lin1 Pri1	-0.6	-0.027
2006.360	57.0	1.323	3	Alz3	-1.4	-0.006
normal point speckle/CCD/Hipparcos measurements						
Date	J°	r"	N	Reference	D J°	D r"
1992.200	62.3	1.159	7	WSI6 HIP1	-0.3	0.000
1996.940	60.7	1.250	21	WSI10 Gii1 Mor10	0.4	0.012
2002.050	59.2	1.302	9	WSI8 Mor1 Slm1	0.0	0.006
2006.845	58.1	1.325	2	WSI1 Sca1	-0.2	-0.007
2011.525	57.6	1.358	4	Los2 Sca1 FMR1	0.1	-0.001

The Visual Triple Star ADS 16185 - STF2934

(Continued from page 218)

Irwin A. W., Yang S. L. S., Walker G. A. H., 1996, PASP, 108, 580

Mason, B. D., Douglass, G.G., Hartkopf, W. I., 1999, AJ, 117, 1023

Seymour, D. M., Mason, B. D., Hartkopf, W. I., Wycoff, G. L., 2002, AJ, 123, 1023

Tokovinin, A. A.; Smekhov, M. G., 2002, A&A, 382, 118

Tokovinin, A., 2008, MNRAS, 389, 925

van Leeuwen, F. 2007, Hipparcos, the New Reduction of the Raw Data (New York: Springer) (data obtained from Simbad data base: I/311)

van den Bos, W. H., 1932, CiUO, 86, 261

Zirm, H., 2011, JDSO, 7, 24